TURBULENCE OVER VERY ROUGH SURFACES

Ryan T. Reynolds & **Ian P. Castro**
School of Engineering Sciences,
University of Southampton
Highfield, Southampton SO17 1BJ, UK
r.reynolds@soton.ac.uk
i.castro@soton.ac.uk

ABSTRACT

Very rough 3D surfaces, typical of urban environments, have roughness elements which occupy a significant percentage of the developing boundary layer above. Laboratory wind tunnel measurements over staggered cube arrays have been undertaken to identify the influence of the relative roughness size on this flow. The surface flow around cubic roughness arrays shows strongly three-dimensional behavior, as seen with anisotropic invariant analysis. The strong contributions to the local shear stress from sweep events bringing high momentum fluid down into the cube canopy are not found in smaller roughness cases. The strong shear layer which exists at the top of the cubes (within the roughness sublayer) is strongly dependent on the boundary layer thickness to roughness height ratio. For deeper boundary layers, relatively, the increased range of scales of motion may lead to smaller peak turbulence intensities. Spatial correlation measurements have also shown the influence of the relative boundary layer thickness on the integral length scales in the near-wall region. The streamwise and wall-normal integral length scales derived from spatial correlations initially increase with height over the cubes and then remain constant for large portions of the outer boundary layer. In summary, the local roughness geometry and relative element size play an important role in determining the flow structure and turbulence characteristics over very rough surfaces.

INTRODUCTION

There is increasing interest in the fundamental nature of boundary layers over rough surfaces. Townsend's (1976) similarity hypothesis suggested that at high Reynolds numbers the turbulent flow outside the near-wall region is essentially independent of the wall roughness, but there has been some recent evidence that this may not be true. Krogstad and Antonia (1999) and Antonia and Krogstad (2001), for example, have shown that rough surfaces can substantially affect the turbulence quantities well into the boundary layer beyond the near-wall region. On the other hand, numerical studies by Flores and Jiménez (2004) and laboratory data obtained by Flack and Schultz (2004) suggest that the effects of wall disturbances are confined to a zone near the wall, as originally supposed by Townsend. We here define a very rough surface as one whose characteristic roughness height, h, is a sufficiently large fraction of the total boundary layer depth, δ, that one might intuitively expect the influence of the roughness to extend well beyond the near-wall region, if not throughout the whole flow. In his helpful recent review on rough wall boundary layers, Jiménez (2004) limits his discussion to $\delta/h > 40$, partly no doubt because there is little data available for smaller values. He concludes that in this range the flow always satisfies Townsend's hypothesis.

Quite apart for the various geometrical parameters defining the particular topology of the roughness, if δ/h is small enough it must surly have a role in controlling the extent of the roughness influence. The issue of just how small δ/h must be for the whole flow to be affected, δ/h_{crit} say, has not yet been explicitly addressed but this critical value may well depend on the roughness topology. It may also be different if the flow is fully developed, (e.g. in a channel) as Krogstad et al. (2004) have suggested. In the meteorological context, boundary layer flow over urban surfaces might have $\delta/h > \delta/h_{crit}$, but there is insufficient evidence to allow definitive statements about how the nature of the turbulence differs from that over less rough surfaces. There has also been little attempt to identify eddy structures over such surfaces, despite their importance in processes like scalar transport from sources within the roughness (but note Finnigan's, 2000, review and the studies of Brunet et al., 1994 and Raupach et al., 1996, in the context of plant canopies).

In the context of a longer term program of work on the nature of very-rough-wall boundary layers, starting from the work of Cheng and Castro (2002) and with some later results reported in Castro et al. (2005), this paper presents further data, chosen to help elucidate the turbulence structure in such flows.

EXPERIMENTAL DETAILS

The surface consists of a staggered array of cubes with a plan area density of 25% as seen in Figure 1. The surface is constructed in a subsonic wind tunnel with a four meter fetch enabling measurement to $x/h = 400$ cube dimensions downstream. The spanwise extent of the facility is $y/h = 90$, reducing any side wall influences. The nominal freestream velocity is 10 m/s, yielding a typical value of $\delta^+ = 6200$ (or $h^+ = 440$), where the superscript + denotes quantities normalized with surface skin friction velocity, u_τ, and kinematic viscosity, ν. Details of the roughness sublayer and inertial sublayer depths, the roughness length and zero plane displacement thicknesses, and horizontal averaging of profile statistics can be found in Cheng and Castro (2002).

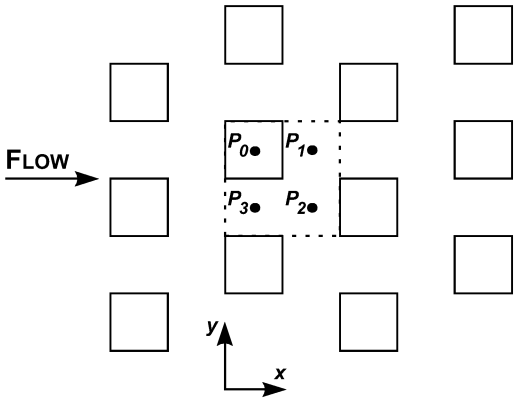

Figure 1: Plan view of the roughness array. Dots labeled $P_0 - P_3$ denote locations of vertical profiles.

The present laboratory work consists of Particle Image Velocimetry (PIV) testing in the boundary layer with special focus on the complicated near surface flow. Additional measurements have been made with Laser Doppler Anemometry (LDA) and Hot Wire Anemometry (HWA) (where appropriate). Velocity time series were obtained in each case with the PIV technique yielding two-dimensional velocity vector maps within the imaging area. Interrogation spots of 16x16 pixels were used with 50% overlap which results in vector spacing of 0.4mm. An adaptive, multi-pass FFT correlation scheme was used to calculate peak displacements. A New Wave Nd:YAG laser illuminated the smoke particles introduced into the flow. The current setup allows PIV measurement within the cube canopy (below the height of the roughness elements) by arranging the camera to look down the streets between the cubes from a side view on a laser light sheet aligned in the streamwise, x, wall-normal, z, plane. Fluorescent paint on the cube surfaces frequency shifts reflected light thereby reducing scattered reflections passing through the narrow band lens filter and into the CCD camera. Data from locations P_1 and P_2 (see Figure 1) are thus obtained within the canopy.

RESULTS

Velocity time series information is used to perform various statistical analysis in order to characterize the structure of the flow over the rough surface. Attention is concentrated on spatial correlations, quadrant analysis of the shear stress, and the stress anisotropy, since these provide some information on structure and are found in some cases to yield results distinctly different from corresponding smooth wall data or, indeed, from rough wall flows with larger δ/h. We start with examples of a quadrant analysis of some of the original time series obtained by Dr. Cheng - the usual statistical quantities were reported in Cheng and Castro (2002). The data were obtained over a staggered array of 20mm cubes, for which δ/h was about 8.0. Quadrant analysis is a local technique yielding information about the instantaneous shear stress transfer (see Lu and Willmarth, 1973). Figure 2 shows the percentage of total shear stress generated by quadrant two events (ejections, Fig.2a) and quadrant four events (sweeps, Fig.2b), compared with data from Krogstad and Antonia (1999), who studied 2D roughness of classical 'k-type', and 3D mesh roughness. In

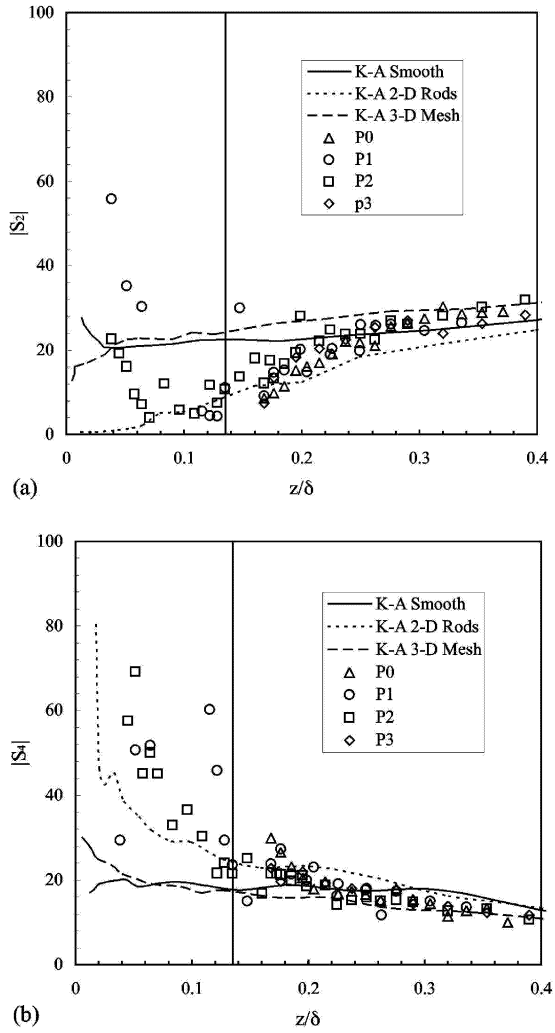

Figure 2: Percentage of total shear stress generated by ejections, $|S_2|$, (a), and sweep, $|S_4|$, (b), plotted against normalized wall distance, z/δ. Vertical lines refer to $z = h$ for the present data. K-A data from Krogstad and Antonia (1999).

both the latter cases, δ/h was much larger (being no less than 26) than in the present case. Note that in all cases the differences in Figure 2 are relatively small for $z/\delta > 0.2$, but in the surface layer the present data shows significant increases in sweep contributions. This occurs largely within the canopy region and the data are therefore, not surprisingly, dependent on particular horizontal location.

An anisotropic invariant map (AIM) deduced from the same data is shown in Figure 3 and is clearly characterized by very low values of -II (the second invariant); all data lies very much closer to the origin than do near-surface data for k-type, 2D roughness, which (close to $z = 0$) lie very close to the upper two-component limit line (see Smalley et al., 2002). This emphasizes the strongly isotropizing influence of the 3D roughness, even deep within the canopy layer. Results like these are discussed in greater detail by Castro et al. (2005).

The strong shear layer above the roughness canopy has been found to be dependent on the relative boundary layer

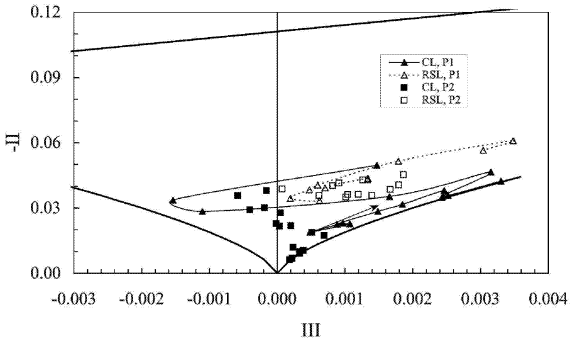

Figure 3: The AIM map for locations P_1 and P_2. The heavy solid lines are segments of the limits of the Lumley triangle. Solid symbols refer to the canopy layer, open symbols the roughness sublayer and the tail of the arrow is near the data point for $z/h = 0.25$ on P_1, with increasing z moving along the line joining the points.

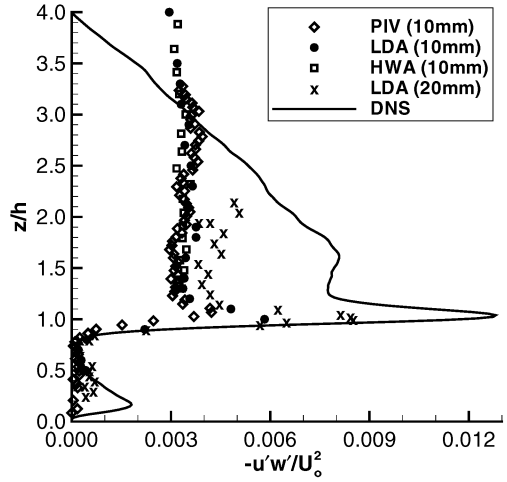

Figure 4: Reynolds shear stress near surface behind cube (P_1). PIV (10mm), $\delta/h = 14$; LDA (10mm), $\delta/h = 14$; HWA (10mm), $\delta/h = 14$; LDA (20mm), $\delta/h = 8$; DNS, $\delta/h = 4$. 20mm LDA data from Cheng and Castro (2002). DNS data from Coceal et al. (2005).

thickness. Stronger velocity gradients are found when the roughness element size protrudes into a significant portion of the boundary layer. The peak in the turbulence intensities and stresses is directly related to the relative roughness size compared to the boundary layer above. As the boundary layer grows, the rough surface occupies a smaller percentage of the boundary layer and smaller shear layers result. This is all illustrated in the data shown in Figure 4 and Figure 5. The former shows the shear stress normalized with the outer velocity scale (free-stream, U_o) for several test cases. Near the cube top surface, $z/h = 1$, the peak in shear stress can be seen to be strongly influenced by the relative boundary layer height, δ/h. The 10mm cases showing PIV, LDA, and HWA data (above the canopy) collapse satisfyingly in the constant shear layer above $z/h = 1.5$ and correspond to a location in which the boundary layer is fourteen times the roughness height. Note that at lower heights the cross-wire data (not shown) are increasingly uncertain because of the high turbulence intensities and that the peak in the LDA data is rather higher than that suggested by the PIV data. This may be a consequence of the lack of adequate spatial resolution in the latter. More importantly, however, the 20mm LDA data (from Cheng and Castro, 2002) reveals a 50% increase in the shear stress peak at $z/h = 1$ for $\delta/h = 8$. A further 50% increase in shear stress at this location is found in DNS data, where $\delta/h = 4$. These DNS data were actually part of a fully resolved channel flow simulation over the cube array by Coceal et al. (2005), so that δ is taken as the channel half-height - the height of the computational domain (and where symmetry conditions were imposed).

This progression in peak shear stress values compared with relative boundary layer depth can be seen in Figure 5. LDA data over 10mm cube arrays were collected at several streamwise locations within the boundary layer and the data from the 20mm LDA cases and the DNS studies (described above) are included. The trend is clear and suggests that a larger relative boundary layer thickness accommodates a greater range

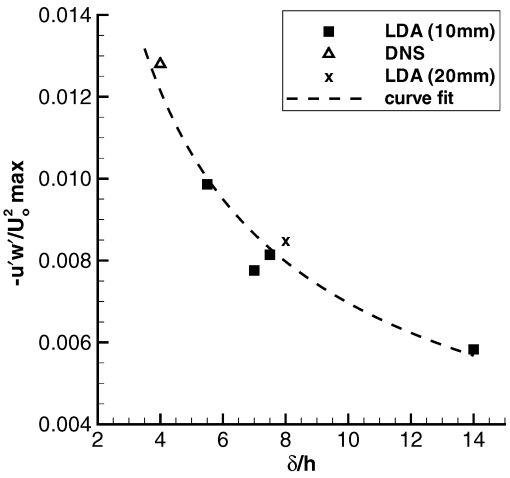

Figure 5: Variation of shear stress peak behind cube (P_1) at $z/h = 1$ with relative boundary layer thickness.

of scales above the canopy, promoting stronger mixing of the shear layer and reducing the shear intensity. It may be, therefore, that the strong 'sheltering' effect of the shear layer just above the canopy, identified by Coceal et al. (2005) and especially apparent in videos of their DNS results, is less effective when there is a much thicker boundary layer region aloft. Currently, these computations are being repeated with a doubled channel height, partly to pursue this point.

Further characterization of the flow structure near the cube surface can be developed with two-point spatial correlation analysis. With the field measurements of PIV data, instantaneous velocity statistics in the streamwise, wall-normal plane (for example) allow for correlation measurements. The spatial

two-point correlation between velocities is here defined in the usual way (equation 1, where σ is the standard deviation of the velocity and Δx is the in-plane separation between measurement locations).

$$R_{uu}(\Delta x) = \frac{\overline{u_1(x,z)u_2(x+\Delta x,z)}}{\sigma_1\sigma_2} \quad (1)$$

Integral length-scales in the flow can be found with this analysis enabling quantification of structure without additional complexities. $R_{uu}(\Delta x)$ was derived from the PIV data at a wall-normal location $z/h = 1.5$ and with the fixed point (subscript 1 in equation 1) centered over a cube (i.e. P_0 in Figure 1). Figure 6 shows the results and includes a similar analysis of the DNS data. As before, the two cases differ in the relative height of the boundary layer. The PIV case corresponds to the laboratory grown wind tunnel boundary layer (present study) which is fourteen times the roughness height. The DNS case (Coceal et al., 2005) is a numerical result under periodic boundary conditions which imposes a fixed outer scale (boundary layer depth) of four times the roughness scale and a periodic horizontal domain of 8x8 cube dimensions. Normalizing the streamwise location with the inner scaling length, h, yields collapse in the data for these two cases only very close to the fixed P_0 location ($\Delta x/h < 0.3$). By introducing a length scale, L_x, defined by assuming the usual (roughly) exponential decay of the streamwise velocity correlation (equation 2), R_{uu}, estimates of the scales can be obtained.

$$R_{uu}(\Delta x) = e^{\frac{-\Delta x/h}{L_x/h}} \quad (2)$$

Note first that in Figure 6 the length scales used to fit the data to the above equation are a factor of three different for the two sets of data, $L_{x2} = 3L_{x1}$, which, interestingly, is nearly the difference in relative boundary layer depths ($\sim$14/4). If an outer scaling, such as the boundary layer thickness, δ, is used, the PIV and DNS data no longer agree for small Δx displacements but are much closer in the outer region. Figure 7 shows the collapse occurring only for $\Delta x/\delta > 0.1$. The existence of two (most dominant) streamwise length scales in the flow above the cube at location P_0 seems quite evident. These can perhaps be explained on the basis of the near-field dominance of structures which scale on the (thin) shear layers separating from the cubes and the far-field dominance of much larger scales, probably similar to those which are well-known, for more standard boundary layers, to produce long correlation tails in the streamwise direction.

If streamwise spatial correlation analysis is performed in a similar way from a datum P_0 location over the cubes at different wall-normal positions, the streamwise length scale variation with height can be found. Figure 8 shows results for the present work. These suggest that initially over the roughness, the length scale grows and becomes constant for a significant portion of the boundary layer, including the outer wake region. Since the PIV data here does not extend to sufficiently large Δx for the correlation to decay to zero, we arbitrarily define a length scale as the width of the profile where the correlation reaches half its maximum ($R_{uu}(\Delta x) = 0.5$). Figure 10 shows the resulting $L_x(uu)$ and it is clear that it first increases for increasing z/h and is then constant for $3.0 < z/h < 10.0$ and only begins to diminish at the outer extremity of the boundary layer where $z/h > 12$ ($z/\delta > 0.85$).

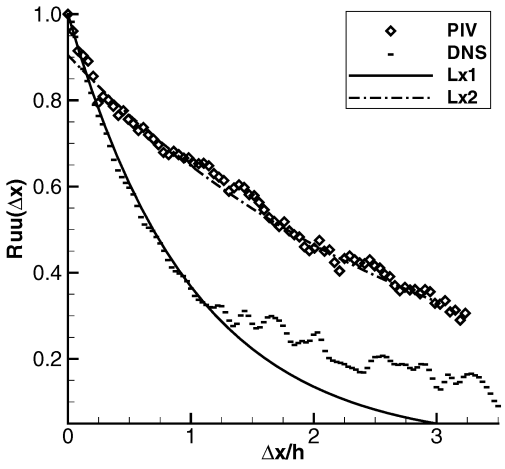

Figure 6: Streamwise spatial correlation normalized with roughness height. At $z/h = 1.5$, with reference centered over cube (P_0). DNS data from Coceal et al. (2005). $L_{x2} = 3L_{x1}$.

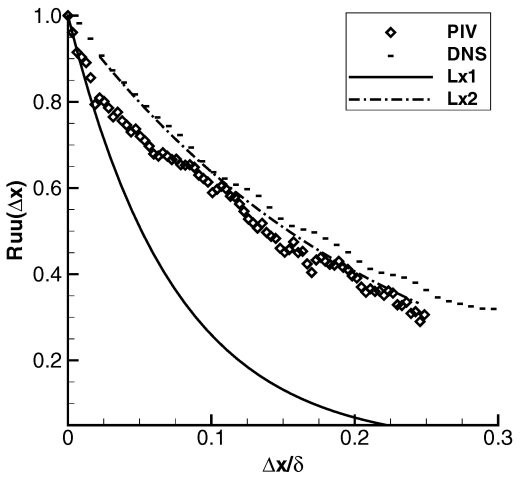

Figure 7: Streamwise spatial correlation normalized with boundary layer height. At $z/h = 1.5$, with reference centered over cube (P_0). DNS data from Coceal et al. (2005). $L_{x2} = 3L_{x1}$.

Corresponding wall-normal velocity spatial correlation results are shown in Figure 9 and indicate that the streamwise coherence in wall-normal velocity fluctuations is short near the surface and grows to a constant value over a majority of the outer portion of the boundary layer. It is also noted that the symmetry of the R_{ww} correlations is skewed slightly, indicating that asymmetric structures are present. Figure 10 includes $L_x(ww)$, deduced from the data in Figure 9 in the same way as for $L_x(uu)$. Notice that the length scales in the streamwise velocity fluctuations are considerably longer (order $\delta/2$) than in the wall-normal velocity fluctuations, as usual in boundary layers. Overall these data suggest that although the cube surface has an isotropizing influence near the surface, large-scale

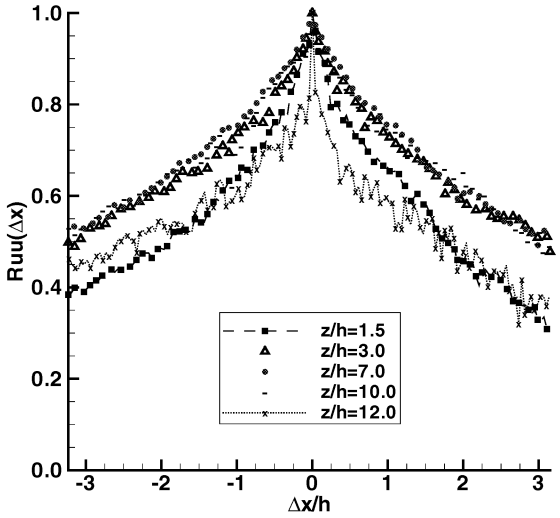

Figure 8: Streamwise velocity, streamwise spatial correlation at several wall-normal locations. At $\delta/h = 14$, with reference centered over cube (P_0).

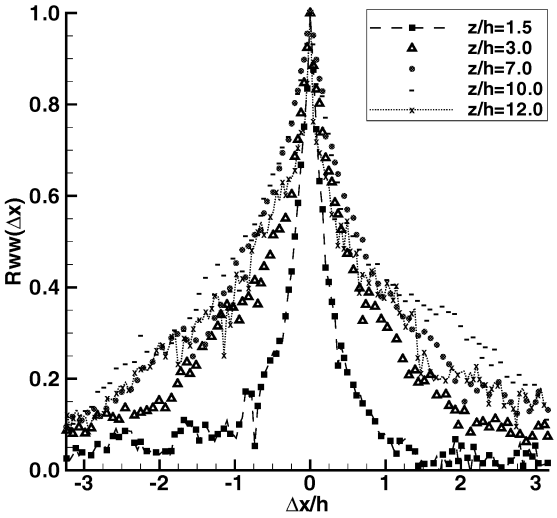

Figure 9: Wall-normal velocity, streamwise spatial correlation at several wall-normal locations. At $\delta/h = 14$, with reference centered over cube (P_0).

coherent streamwise structures remain present in the flow and are perhaps not too dissimilar from those in regular boundary layers. Ganapathisubramani et al. (2005), to give a recent example, measured spatial correlations in smooth wall turbulent boundary layers in an effort to support structural theories of the hairpin vortex packet model. Their work, using 3D PIV, characterized the streamwise length scale development with height in the boundary layer and they found that in the log-law region the length scale increases with height, but decreases in the outer wake region. The present correlation behavior suggests structures which are perhaps only marginally different than those reported by Ganapathisubramani et al., but further work is needed to clarify any detailed differences. In particular, we intend determining average structure angles by obtaining complete correlation contours in the vertical $(x - z)$ plane, to compare with those obtained by Castro et al. (2005) in similar flows but having much smaller h/δ.

CONCLUSIONS

It is clear that more research into the flow behavior of very-rough-wall boundary layers is required. Results reported here suggest features which are both different and, in other respects, similar to those in boundary layers with smaller roughness or, indeed, in smooth-wall flows.

Quadrant analysis of the Reynolds shear stress and corresponding AIM maps have shown agreement with other rough wall studies but emphasized the strong sweep events and heterogeneous nature of the flow near the surface. The strong tendency towards isotropy of the flow near to and within the canopy is evident with AIM analysis. It has been shown that the relative boundary layer thickness, δ/h, influences the strength of the shear layer just above the canopy and perhaps also the integral spatial length scales present. Numerical studies with compromised domain sizes must take these factors into consideration. The development of streamwise coherence, interpreted with spatial correlation analysis, has shown near constant length scales for $0.2 < z/\delta < 0.8$ with streamwise

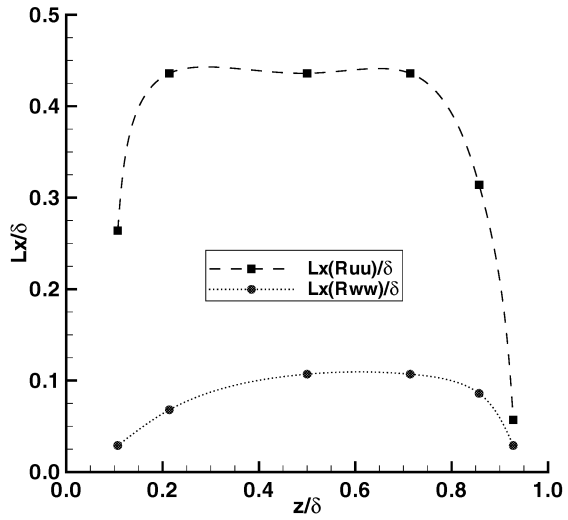

Figure 10: Streamwise length scale variation with boundary layer height for streamwise and wall-normal velocity fluctuations. At $\delta/h = 14$, with reference centered over cube (P_0).

velocity scales being significantly longer than wall-normal velocity scales, as usual. The constant nature of the correlation results in the outer layer seems to differ somewhat from similar studies over smooth wall layers.

The authors gratefully acknowledge support from the Natural Environment Research Council (NERC) through their UWERN program (DST/26/39) and wish to thank Dr. Omduth Coceal for the use of his DNS data.

REFERENCES

Antonia, R.A. and Krogstad, P.Å., 2001, "Turbulence structure in boundary layers over different types of surface roughness," *Fluid Dyn. Res.,* 28, pp. 139-157.

Brunet, Y., Finnigan, J.J., and Raupach, M.R., 1994, "A wind tunnel study of air flow in waving wheat: single-point velocity statistics," *Boundary Lay. Met.,* 70, pp. 95-132.

Castro, I.P., Cheng, H., and Reynolds, R.T., 2005, "Turbulence over urban roughness: deductions from wind tunnel measurements," *Boundary Lay. Met.,* in press.

Cheng, H. and Castro, I.P., 2002, "Near wall flow over urban-like roughness," *Boundary Lay. Met.,* 104, pp. 229-259.

Coceal, O., Thomas, T.G., Castro, I.P., Belcher, S.E., 2004, "Numerical simulation of turbulent flow over cubic roughness arrays," *J. Fluid Mech.,* submitted.

Finnigan, J., 2000, "Turbulence in plant canopies," *Annu. Rev. Fluid Mech.,* 32, pp. 519-571.

Flack, K.A. and Schultz, M.P., 2004, "Turbulence structure over two types of uniform roughness," *Advances in Turbulence X,* ed. Andersson, H.I. and Krogstad, P.Å., pp. 281-284.

Flores, O. and Jiménez, J., 2004, "Effect of wall boundary disturbances on turbulent channel flow," *Advances in Turbulence X,* ed. Andersson, H.I. and Krogstad, P.Å., pp. 235-238.

Ganapathisubramani, B., Hutchins, N., Hambelton, W.T., Longmire, E.K, and Marusic, I., 2005, "Investigation of large-scale coherence in a turbulent boundary layer using two-point correlations," *J. Fluid Mech.,* 524, pp. 57-80.

Jiménez, J., 2004, "Turbulent flows over rough walls," *Annu. Rev. Fluid Mech.,* 36, pp. 173-196.

Krogstad, P.Å. and Antonia, R.A., 1999, "Surface roughness effects in turbulent boundary layers," *Expt. in Fluids,* 27, pp. 450-460.

Lu, S.S. and Willmarth, W.W., 1973, "Measurements of the structure of the Reynolds stresses in a turbulent boundary layer," *J. Fluid Mech.,* 60, pp. 472-478.

Raupach, M.R., Finnigan, J.J., and Brunet, Y., 1996, "Coherent eddies and turbulence in vegetation canopies: the mixing layer analogy," *Boundary Lay. Met.,* 78, pp. 351-382.

Smalley, R.J., Leonardi, S., Antonia, R.A., Djenidi, L., and Orlandi, P., 2002, "Reynolds stress anisotrophy of turbulent rough wall layers," *Expt. in Fluids,* 33, pp. 31-37.

Townsend, A.A., 1976, *The structure of turbulent shear flow,* Cambridge Uni. Press, Cambridge.